Influence of the System Geometry on the Characteristics of the Surface Tension Auto-oscillations: A Numerical Study

N. M. Kovalchuk[†] and D. Vollhardt*[,‡]

Max-Planck-Institute of Colloids and Interfaces, 14424 Potsdam/Golm, Germany, and Institute for Problems of Material Science, 03142 Kiev, Ukraine

Received: October 28, 2002

A numerical study of the processes that occur in a small cylindrical vessel with rigid walls, by the dissolution of a surfactant droplet placed on the capillary tip under the free water interface, is presented. Periodically arising Marangoni instability reveals itself in auto-oscillations of the surface tension. The effect of geometrical factors—namely, capillary immersion depth, capillary and droplet radii, and container height and radius—on the auto-oscillation characteristics is analyzed. The numerical and experimental results are compared and discussed.

Introduction

Auto-oscillation of surface tension is one of the most impressive manifestations of self-organization in systems far from equilibrium.[1,2] The phenomenon can be observed using a rather simple experimental setup.[3,4] Namely, a droplet of a limited soluble surfactant (such as, for example, an aliphatic alcohol or a fatty acid) can be placed on the tip of a capillary in a vessel that has been filled with pure water. Well-shaped regular oscillations of the surface tension develop at the air−water interface after some induction time. The oscillations have an asymmetrical shape, with an abrupt decrease of the surface tension, followed by its gradual increase. The decrease in the surface tension is accompanied by fast surface movement from the capillary to the vessel wall. The motion dampens after a rather short time, when the surface tension begins to increase. The analysis of the system behavior has shown that the auto-oscillations can be explained on the basis of Marangoni instability, which periodically arises and fades in the system.[5−7] The evolution in systems governed by Marangoni instability are widely studied; however, questions still remain concerning the mechanism of instability, which arises in cases where nonlinear oscillations occur by mass transfer.[8−12] A comprehensive study of the auto-oscillation of the surface tension can be useful for a better understanding of these nonlinear phenomena.

A first analysis of the mechanism for the development of repeated surface tension auto-oscillations driven by the Marangoni force has been performed in ref 7. At the beginning of the droplet dissolution, only diffusion mass transfer occurs in the system. When some amount of surfactant reaches the air−water interface, convection that is due to a surface concentration gradient begins to develop. The circular convective flow supplies an additional amount of surfactant to the interface in the region above the capillary. That leads to an increase of the surface concentration gradient and an intensification of the convection. Therefore, there is feedback in the system under consideration, which leads to the development of instability. However, only when the normal concentration gradient near the surface becomes large enough does instability develop in the system, resulting in a very fast increase of the surface and bulk velocity. Convection brings the surfactant to the surface in the vicinity of the capillary and spreads it over the surface. An abrupt decrease of the surface tension is observed at this time. At a certain moment in time, the amount of surfactant supplied to the surface becomes insufficient to support the large velocity, and the instability fades.

There are two possible ways for the succeeding evolution of the system, depending on the geometry of the system.[7] The velocity can decrease up to a rather small value, whereupon it increases very slowly. Correspondingly, the surface tension initially increases and then slowly decreases. This is the case when only a single oscillation appears in the system. The possibility of repeated oscillations is related to the interaction of the concentration wave on the surface with the container wall. The surface contraction near the wall causes the appearance of a surface concentration gradient directed opposite the capillary. The surface velocity decreases fast at the wall, and then the liquid begins to move in the direction opposite to the capillary. As a result, the moving liquid forms two convective rolls that rotate in opposite directions (one is located near the capillary and other is located near the wall). Interaction of these rolls leads to a fading of convection, because of viscous dissipation. The return of the system to a slow diffusion stage is the precondition for the appearance of the following oscillation. Obviously, the intensity of the direct and opposite convective rolls is dependent on the distance between the capillary and wall, on the capillary immersion depths, etc.; therefore, the system geometry is very important for the phenomenon of auto-oscillations of the surface tension.

A common object for the observation of Marangoni instability is a liquid layer with a gradient of temperature or concentration that is imposed perpendicular to the free surface or along it.[2] When the ratio of the characteristic horizontal and vertical dimensions (aspect ratio) is on the order of unity, the instability development is strongly dependent on the system geometry.[13−18] The selection of the flow pattern is related to the aspect ratios in experiments with confined geometry. Moreover, a decrease of the aspect ratio leads to the system stabilization, i.e., to an increase of the critical value of the Marangoni number (Ma).

* Author to whom correspondence should be addressed. E-mail: vollh@mpikg-golm.mpg.de.
[†] Max-Planck-Institute of Colloids and Interfaces.
[‡] Institute for Problems of Material Science.

10.1021/jp022321y CCC: $25.00
Published on Web 07/29/2003

The effect of aspect ratio also should be expected in the case of surface tension auto-oscillations. This is confirmed by the presented analysis.

The objective of the present study is to clarify the effect of different geometrical factors on the development and characteristics of the auto-oscillations of the surface tension. Because of the peculiarities of the concentration distribution in the system where auto-oscillation of the surface tension occurs, the conditions for the creation of instability emerge, at first, only in the vicinity of the capillary and cannot be essentially influenced by the vessel diameter and the aspect ratio. In contrast, the presence of the lateral wall is crucial for the fading of instability as a precondition for the development of repeated oscillations. The auto-oscillations should be observable in containers with small aspect ratios, rather than in those with large aspect ratios. It also has been confirmed experimentally that the characteristics of the auto-oscillations of surface tension, as well as their appearance, are dependent strongly on the system geometry.[4,19] Repeated oscillations do not develop when the aspect ratio of the vessel is larger than a certain critical value. In the present study, numerical simulations about the behavior of model systems, which are similar to the experimental systems, are performed for different cell dimensions, capillary immersion depths, and radii of the capillary and droplet. This examination will help to understand the auto-oscillation mechanism in more detail.

Mathematical Formulation

A full description of the mathematical model and the numerical scheme used in the numerical simulations is given in ref 7. Therefore, we present only the most-important features here.

The geometry of the model system used for the numerical study is chosen according to the experimental conditions of ref 4. The model system is a cylindrical container that is filled with a viscous, incompressible Newtonian liquid (namely, water). The upper free-liquid surface is in contact with a passive gas. A cylindrical capillary with a spherical surfactant droplet on the tip is situated in the liquid so that the capillary axis coincides with the container axis.

The system evolution is governed by a set of nonlinear and nonstationary equations: Navier−Stokes and continuity and convective diffusion equations. According to the system symmetry, a cylindrical coordinate system is used. The radial direction is obviously preferred for the development of convection on the surface. The experimental observations confirm that there is no noticeable surface motion in the azimuthal direction, which is why the dependency on the azimuthal coordinate is neglected. In this case, the governing equations can be rewritten in terms of vorticity and stream function, and the pressure can be eliminated from the Navier−Stokes equations.

By scaling time, length, velocity, concentration, stream function, and vorticity correspondingly with L^2/D, L, D/L, c_0, LD, D/L^2, the dimensionless form of the governing equations is given as

$$\frac{\partial\omega}{\partial t}+\frac{\partial(v_r\omega)}{\partial r}+\frac{\partial(v_z\omega)}{\partial z}-\mathrm{Sc}\left(\frac{\partial^2\omega}{\partial r^2}+\frac{\partial^2\omega}{\partial z^2}+\frac{1}{r}\frac{\partial\omega}{\partial r}-\frac{\omega}{r^2}\right)=0 \quad (1)$$

$$\frac{\partial^2\Psi}{\partial r^2}+\frac{\partial^2\Psi}{\partial z^2}-\frac{1}{r}\frac{\partial\Psi}{\partial r}-\omega r=0 \quad (2)$$

$$\frac{\partial c}{\partial t}+\frac{\partial(v_r c)}{\partial r}+\frac{\partial(v_z c)}{\partial z}+\frac{v_r c}{r}-\left(\frac{\partial^2 c}{\partial r^2}+\frac{\partial^2 c}{\partial z^2}+\frac{1}{r}\frac{\partial c}{\partial r}\right)=0 \quad (3)$$

where L is the characteristic length scale, D the bulk diffusion coefficient of the surfactant, c_0 the surfactant solubility, t the time, r the radial coordinate, and z the normal to the interface coordinate directed downward with $z = 0$ on the interface. The velocity components in the radial direction and normal to the interface are v_r and v_z, respectively; Ψ is the stream function, which is defined such that $v_r = (1/r)(\partial\Psi/\partial z)$ and $v_z = -(1/r)(\partial\Psi/\partial r)$; ω is the vorticity ($\omega = (\partial v_r/\partial z) - (\partial v_z/\partial r)$), Sc is the Schmidt number ($\mathrm{Sc} = \nu/D$); ν is the kinematic viscosity of the liquid; and c is the surfactant concentration.

The governing equations are solved using the appropriate initial and boundary conditions. In the initial state, the liquid is supposedly motionless. The dimensionless surfactant concentration is equal to unity at the droplet/water interface and is equal to zero elsewhere. It is also supposed that the densities of the solute and solvent are equal to each other, and, therefore, the buoyancy effect is not considered. No-slip boundary conditions are used for the container wall and bottom, for the capillary, and for the droplet surface.

The free air−liquid interface is assumed to be nondeformable, and its intrinsic viscosity as well as evaporation are neglected. Diffusion-controlled adsorption kinetics is assumed. The mass balance on the free surface is described by the following equation:

$$\frac{\partial\Gamma}{\partial t}+\frac{\partial(\Gamma v_r)}{\partial r}+\frac{\Gamma v_r}{r}-\frac{D_s}{D}\left(\frac{\partial^2\Gamma}{\partial r^2}+\frac{1}{r}\frac{\partial\Gamma}{\partial r}\right)-\frac{L}{K_L\Gamma_m}\frac{\partial c}{\partial z}=0 \quad (\text{at } z=0) \quad (4)$$

Here, K_L and Γ_m are the parameters of the Langmuir isotherm, D_s is the surface diffusion coefficient, and Γ is the Gibbs adsorption (scaled by $c_0K_L\Gamma_m$).

Two new dimensionless parameters appear in the boundary condition described in eq 4. The parameter D_s/D determines the contribution of the surface diffusion to the change in the surface concentration. Kovalchuk and co-workers[5,6] showed that, for a semi-infinite liquid layer, the surface diffusion mass transfer is rather small, and a change of the value of D_s/D in the limit of 1−1000 practically has no influence on the induction time and the characteristics of the first oscillation. Also, considering the lack of the authentic data concerning the surface diffusion coefficients of the organics in water, we accept D_s/D to be equal to unity in the following calculations.

The last term in eq 4 corresponds to the normal diffusion flux to the surface. The dimensionless parameter, which appears here, is the ratio of the characteristic length scale for the system considered to the characteristic adsorption length $K_L\Gamma_m$. It is obvious that L is of the order of 1 cm for the considered system, and, therefore, the relation $L/K_L\Gamma_m \gg 1$ is always valid.

Another dimensionless parameter, the Marangoni number ($\mathrm{Ma} = \mathrm{R}Tc_0K_L\Gamma_mL/(\rho\nu D)$, where R is the gas constant, T the temperature, and ρ the liquid density), appears in the boundary condition for the vortex on the free surface:

$$\omega=\mathrm{Ma}\frac{1}{1-K_Lc_0\Gamma}\frac{\partial\Gamma}{\partial r} \qquad (\text{at } z=0) \quad (5)$$

The condition of eq 5 is obtained from the tangential stress balance on the free surface, using the Szyszkowsky−Langmuir equation for the surface tension.

Numerical simulations were performed using the finite difference method on a regular grid with a resolution of 0.0125 for the following surfactant properties: solubility, $c_0 = 3.4$ mol/m^3; parameters of the Langmuir isotherm, $K_L = 3.23$ m^3/mol, $\Gamma_m = 6.6 \times 10^{-6}$ mol/m^2; and volume and surface diffusion

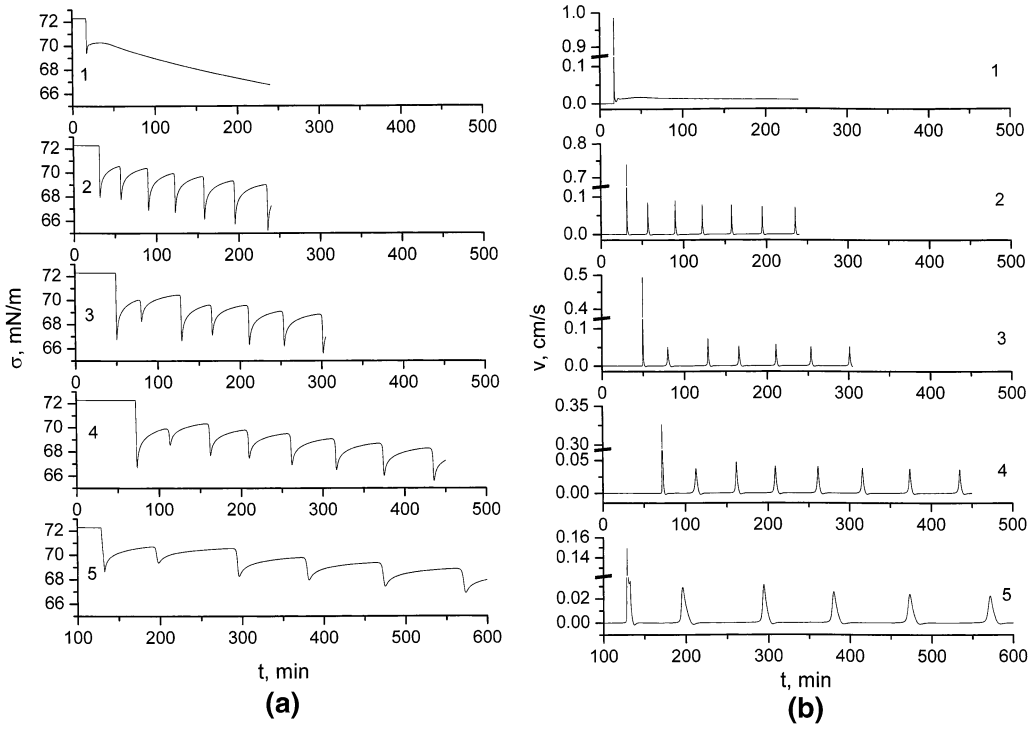

Figure 1. Graphical depictions of (a) surface tension σ versus time t and (b) surface velocity v versus time t for different capillary immersion depths: $h = 6$ mm (curve 1), 8 mm (curve 2), 10 mm (curve 3), 12 mm (curve 4), and 16 mm (curve 5). Calculations were made for a cell radius of $R = 20$ mm and a height of the liquid layer of $H = 20$ mm.

TABLE 1: Dependence of the Auto-oscillation Characteristics on the Immersion Depth of the Capillary

		Oscillations		Velocity,[b] mm/s	
h, mm	induction period, min	period,[a] min	amplitude,[b] mN/m	maximum positive value	maximum negative value
6	17		2.9/-	9.8/-	
8	31	35	4.3/3.4	7.4/0.81	0.013/0.0176
10	49	43	5.5/3.1	4.9/0.58	0.015/0.0166
12	72	53	5.6/2.5	3.3/0.42	0.0175/0.0140
16	128	92	3.6/2.0	1.5/0.27	0.0168/0.0108

[a] Mean value for the third to sixth oscillations. [b] Value in numerator represents that for the first oscillation, whereas the value in the denominator represents the mean value for the third to sixth oscillations.

coefficients, $D = D_s = 6.7 \times 10^{-10}$ m^2/s. These properties are similar to those for octanol.

There are five geometrical parameters that can affect the system behavior: the radius of the container (R), the height of the liquid layer (H), the capillary immersion depth (h), the capillary radius (r_c), and the droplet radius (r_0). To study their effects, we changed each of these parameters, keeping the other parameters constant, as follows: $R = 20$ mm, $H = 20$ mm, $h = 8$ mm, $r_c = 1$ mm, $r_0 = 1.5$ mm. The characteristic length scale is chosen in accordance to the vessel dimensions ($L = 20$ mm). The values of the surface tension and surface velocity, given in the next section, are calculated for the distance $r = 10$ mm from the capillary axis.

Results and Discussion

Capillary Immersion Depth. The dependence of the auto-oscillation characteristics on the capillary immersion depth is presented in Figure 1 and Table 1. The simulations show that the characteristics of the first and subsequent oscillations are different, so they are given separately in Table 1. Solely, a single oscillation appears when the capillary immersion depth is less than its critical value ($h = 6$ mm). Repeated oscillations occur for capillary immersion depths of $h \geq 8$ mm. The induction period (the time when the surface tension is almost constant, up to the first oscillation) and the oscillation period increase, whereas the amplitudes of the second and subsequent oscillations decrease as the immersion depth of the capillary increases. The oscillation period is dependent less significantly on the capillary immersion depth than the induction period, because of surfactant mixing in the bulk and a local increase of the convective contribution to the mass transfer (namely, in the capillary region) after the first oscillation. The dependence of the amplitude of the first oscillation on the immersion depth is more complicated.

Consider first the system behavior during the induction period. A comprehensive analysis of the mass transfer kinetics at this time has been performed in refs 5 and 7. Initially, the liquid is motionless and the solute from the droplet is distributed over the bulk by means of diffusion. The convection due to the Marangoni effect develops in the system when some small amount of the solute reaches the surface. The contribution of convection to the mass transfer increases with time and becomes predominant when instability occurs.

Given that convection occurs in the system during practically the entire induction period, the question is: How large is its influence on the system evolution? Simple calculations show that the values of the induction period given in Table 1 are almost proportional to the square of the capillary immersion depth, which points to the diffusion kinetics of the mass transfer during this time. Figure 2 gives another illustration of the negligible role of the convection in the mass transfer during the induction period. Curve 1 in Figure 2 reflects the results of the numerical simulation presented in Figure 1 for $h = 10$ mm. Curve 2 in Figure 2 corresponds to pure diffusion mass transfer for the same depth (the results are obtained by the formal acceptance of $Ma = 0$). Both curves practically coincide during the entire induction period. Thus, the induction period is the

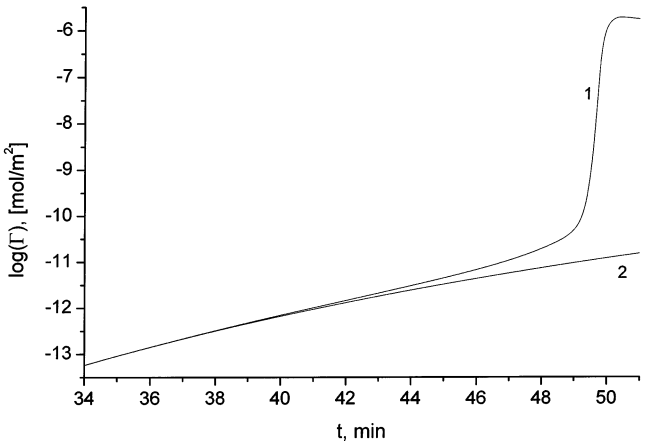

Figure 2. Surface concentration versus time near the capillary during the induction period and at the beginning of the first oscillation: curve 1 considers both convective and diffusion mass transfer, whereas curve 2 considers only pure diffusion mass transfer. Capillary immersion depth was $h = 10$ mm, the cell radius was $R = 20$ mm, and the height of the liquid layer was $H = 20$ mm.

diffusion stage in the system evolution and convection can be neglected at this time.

In addition, another simulation was also performed, under the assumption that convection is absent in the system until the surface concentration near the capillary is $<10^{-11}$ mol/m^2 (which means up to the beginning of the increase of instability, according to Figure 2). The calculation shows that the system behavior does not differ from that obtained for a system where convection occurs constantly. The only difference is a small, insignificant increase in the induction period. At the same time, when the velocity distribution corresponding to the time of the instability increase is combined with the concentration distribution at the beginning of the droplet dissolution, the velocities dampen within some minutes and the system returns to the state dominated by diffusion. These numerical experiments clearly show that instability develops in such a system only after reaching concentration gradients that are sufficiently high. Particularly, the concentration gradients in the solution below the interface are crucial for the development of instability, and the velocity values that are attained in the system at the end of the induction period have only a minor role.

The presented simulation results can also be helpful for the understanding of the effect of adsorption kinetics on the development of nonlinear oscillations development. In a recent paper, the role of adsorption kinetics was discussed by Takahashi et al. by assuming an adsorption barrier.[12] They generated a single surface tension oscillation at the water−nitrobenzene interface, because of sodium dodecyl sulfate (SDS) transfer. An amount of SDS was injected with a microsyringe in a point of the water bulk far from the water−nitrobenzene interface. When SDS reaches the interface, this system reveals a single oscillation, which obviously resembles the oscillation studied here. It is supposed in ref 12 that the surfactant adsorption is hindered during the induction period by a barrier-like effect at the liquid−liquid interface and drastic adsorption occurs after the concentration at the "sub-interface" region reaches a threshold value. This assumption was made because no remarkable changes in the surface tension were observed, whereas the subsequent decrease in the surface tension was very sharp.

Our simulations reveal clearly that a constant surface tension (within the experimentally reasonable limits) during the induction period is realized in the framework of a simple model where diffusion-limited adsorption kinetics is accepted without any barrier-like effects. Figure 2 shows that a gradual increase of the surface concentration occurs in the system during the induction period, but its values remain too small to produce detectable changes in surface tension. The subsequent sharp decrease of the surface tension is caused by a fast-developing convection and not by drastic adsorption of the surfactant accumulated at a "sub-interface". Note that the critical concentration gradient is formed not in an infinitely thin "sub-interfacial" layer but rather in a macroscopically large region (in our case, between the drop and the interface). Thus, there is no necessity to assume the possibility of barrier-like effects for adsorption in the considered systems.

The development of instability manifests itself in a rapid increase of the surface velocity (Figure 1b). The velocity is zero on the wall and on the capillary; therefore, surface extension occurs near the capillary and surface contraction occurs near the wall. The latter leads to an increase of the surface concentration near the wall, in comparison to the adjacent parts of the surface and to the formation of a concentration gradient directed toward the capillary (reversed surface concentration gradient). When the supply of surfactant near the capillary becomes insufficient to support the velocity growth, this reverse gradient causes a decrease of the surface velocity and the instability fades. If the reverse concentration gradient is large enough, it causes surface motion in the reverse direction (to the capillary). In this case, two convective rolls coexist in the system, rotating in opposite directions (Figure 3). The velocities in both rolls decrease very fast, because of viscous dissipation. The system returns to the slow stage, where the diffusion transfer is significant. This is a precondition for the development of the subsequent oscillations.[7]

To characterize the growth rate of the velocity, we calculated the time scale t_g for various capillary immersion depths; t_g is defined as the time when the surface velocity increases from $0.1v_{max}$ to v_{max} (see Table 2). The decay rate of the velocity is characterized by the time scale t_d, which is defined as the time when the velocity decreases from v_{max} to $0.1v_{max}$. Another characteristic time, t_c, which corresponds to the time required to increase the surface concentration from $0.6c_{max}$ to c_{max}, is chosen, because of the fact that the concentration changes during the oscillation almost two times. Finally, the value t_i corresponds to the entire time of the surface concentration increase during the oscillation. It should be stressed that the surface concentration increases during a certain time after the velocity already begins to slow, and then it decreases too. Table 2 shows that the characteristic times are dependent strongly on the capillary immersion depth. They increase as the capillary immersion depth increases. Thus, it can be concluded that all the processes become slower as the immersion depth of the capillary increases.

Deceleration of the processes in the system, relative to the increasing immersion depth of the capillary, is also confirmed by the values of the surface velocity given in Table 1. There is only one exception: the maximum negative velocity after the first oscillation increases as the immersion depth of the capillary increases from 8 mm to 12 mm. This effect is related to the absence of repeated oscillations at small immersion depths of the capillary. As already noted, the development of the liquid motion from the wall to the capillary (negative velocities) is the necessary precondition for the development of repeated oscillations. It is obvious that the larger the positive velocity, the larger the surface contraction near the wall and the larger the reverse surface concentration gradient. However, the increase in the reverse concentration gradient does not seem to be sufficient to counteract the inertia of the direct flow at large

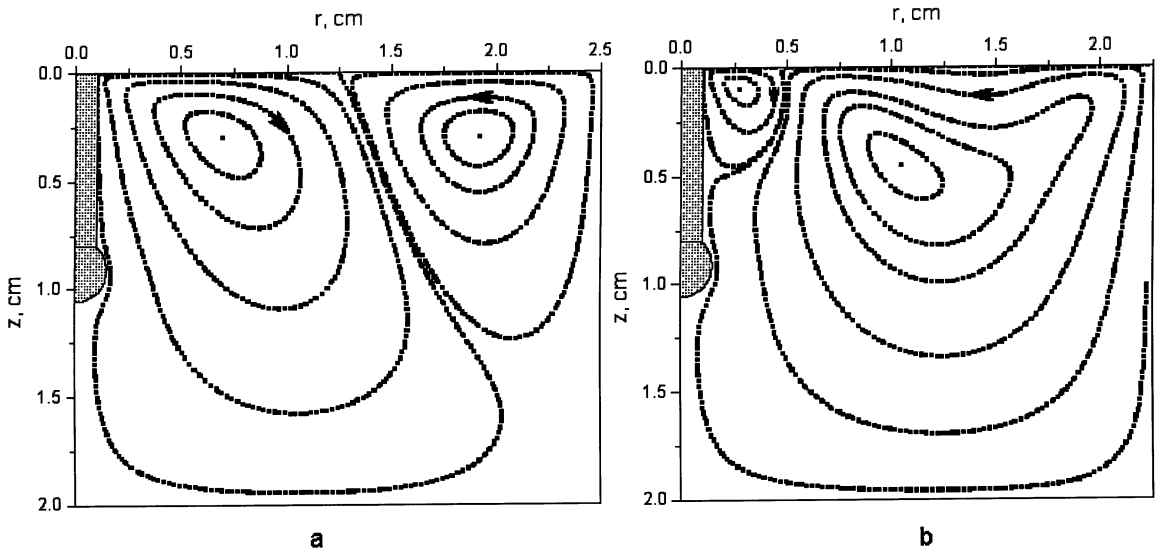

Figure 3. Stream lines distribution in the bulk after the first oscillation for $H = 20$ mm, $h = 8$ mm, and (a) $R = 25$ mm, or (b) $R = 22.5$ mm.

TABLE 2: Characteristic Time Scales, Depending on the Immersion Depth of the Capillary

	Time Scale,[a] s			
h, mm	t_g	t_d	t_c	t_i
6	5/-	6/-	22/-	35/-
8	7/40	14/75	22/31	40/143
10	12/88	35/115	23/53	58/220
12	18/167	84/180	48/95	109/324
16	39/322	142/445	99/408	302/621

[a] Value given in the numerator represents that for the first oscillation, whereas the value given in the denominator represents the mean value for the subsequent fourth to sixth oscillations.

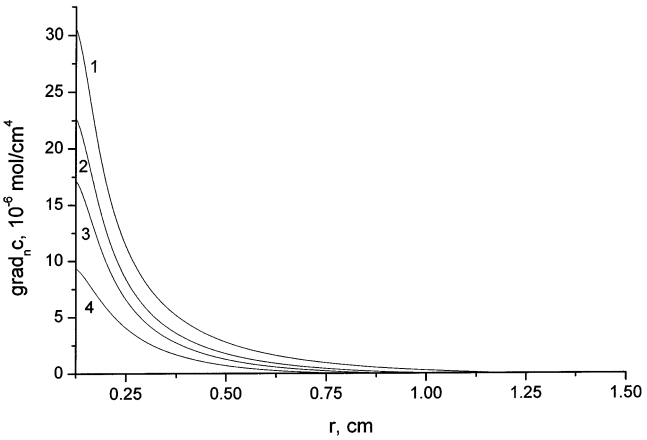

Figure 4. Radial distribution of the normal concentration gradient near the surface, depending on the capillary immersion depth: curve 1, $h = 8$ mm, t = t* + 195 min, 15 s; curve 2, $h = 10$ mm, t = t* + 254 min, 9 s; curve 3, $h = 12$ mm, t = t* + 316 min, 53 s; and curve 4, $h = 16$ mm, t = t* + 574 min, 31 s. Calculations were made for a cell radius of $R = 20$ mm and the height of the liquid layer was $H = 20$ mm; all data are for the sixth oscillation.

positive velocities. For velocities that are small enough positive, this gradient is sufficient to force the liquid movement in the opposite direction, and, moreover, the larger the positive velocity, the larger the corresponding negative velocity (cf. $h = 16$ mm and $h = 12$ mm). However, at more positive velocities, the influence of the reverse concentration gradient becomes smaller, and the negative velocity decreases as the positive velocity increases (cf. $h = 12$ mm, $h = 10$ mm, and $h = 8$ mm). Finally, when the positive velocity exceeds a critical

TABLE 3: Dependence of Auto-oscillation Characteristics on the Cell Radius

			Oscillations		Velocity,[b] mm/s	
R, mm	h, mm	induction period, min	period,[a] min*	amplitude,[b] mN/m	maximum positive value	maximum negative value
12	8	31	46	6.0/3.6	1.6/0.081	0.0086/0.0067
20	8	31	35	4.3/3.4	7.4/0.81	0.013/0.0176
22.5	8	31	33	3.4/2.9	8.9/1.12	0.0098/0.0156
25	8	31		2.7/-	9.6/-	-/-
30	8	31		1.8/-	10.9/-	-/-
20	12	72	53	5.6/2.5	3.3/0.42	0.0175/0.0140
25	12	72	47	4.4/2.2	4.9/0.82	0.0153/0.0136
30	12	72	44	3.0/1.6	6.3/1.3	0.0143/0.0106

[a] Mean value for the third to sixth oscillations. [b] Value given in the numerator represents that for the first oscillation, whereas the value in the denominator represents the mean value for the third to sixth oscillations.

value, the reverse concentration gradient becomes insufficient to force the liquid motion in the opposite direction ($h = 6$ mm). This is a case when only a single oscillation can be observed.

The supply of surfactant to the interface at any moment in time is determined by the normal concentration gradient near the interface. The radial distribution of the normal concentration gradient for the sixth oscillation is presented in Figure 4. The time chosen for each capillary immersion depth corresponds to the moment when the gradient reaches its maximum. The normal gradient and the rate of its growth with time decrease as the capillary immersion depth increases. The total amount of surfactant delivered to the interface during the oscillation is dependent on the values of the normal concentration gradient, on the surface area to which the surfactant is supplied, and on the duration of the time interval when the surfactant is supplied to the interface. The first two factors decrease as the capillary immersion depth increases. However, the time during which surfactant is delivered increases. The joint action of the three factors results in the observed dependency of the oscillation amplitude for the first oscillation on the capillary immersion depth, which was noted previously (see Table 1). At the same time, the amplitudes of the subsequent oscillations decrease as the capillary immersion depth increases.

Cell Radius. The effect of the cell radius on the system evolution was studied for two capillary immersion depths: h

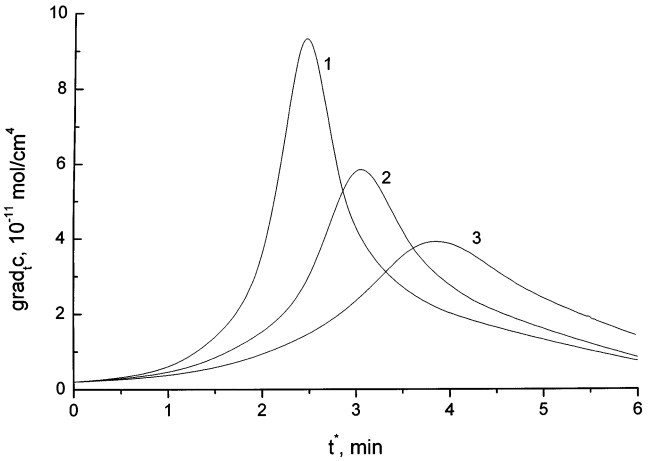

Figure 5. Tangential concentration gradient at the surface ($r = 10$ mm) versus time t^*, depending on the cell radius: curve 1, R = 30 mm, $t = t^* + 283$ min, 28 s; curve 2, $R = 25$ mm, $t = t^* + 295$ min, 54 s; and curve 3, $R = 20$ mm, $t = t^* + 312$ min. Calculations were made for the capillary immersion depth $h = 12$ mm and the height of the liquid layer $H = 20$ mm; all data are for the sixth oscillation.

$= 8$ mm and $h = 12$ mm. The results of the simulations are presented in Table 3.

The increase of the cell radius leads to an increase of the maximum surface velocities for both depths. The effect is more pronounced for cell radii that are sufficiently small. The values of the surface velocities attained in the system are dependent on both the tangential concentration gradient at the surface and the bulk velocity distribution (due to tangential stress balance). Figure 5 shows that the maximum tangential concentration gradient attained in the system increases as the cell radius increases, similar to the relationship with velocity. The similarity in the behavior of the tangential concentration gradient and that of the surface velocity is observed also when other geometrical parameters are changed. Thus, the surface velocities are mainly determined by the tangential concentration gradients. The differences in the bulk velocity distributions are not crucial for the surface velocity. At the same time, the ratio of the maximum of the surface velocity and the maximum of the tangential concentration gradient at the same point of the surface changes with the alteration of the system geometry. For example, it increases as the cell radius increases. Moreover, this ratio is dependent on the radial coordinate in the fixed system. This result shows that inertia is also a significant factor and defines the surface velocity, especially in the regions far from the capillary, where the tangential surface concentration gradients are smaller, because the supply of surfactant from the bulk is absent here.

As discussed previously, repeated oscillations occur in the system, provided that the surface velocity at the onset of instability after the induction period is smaller than a certain critical value. When the cell radius and, correspondingly, the velocity exceed the respective critical values, only a single

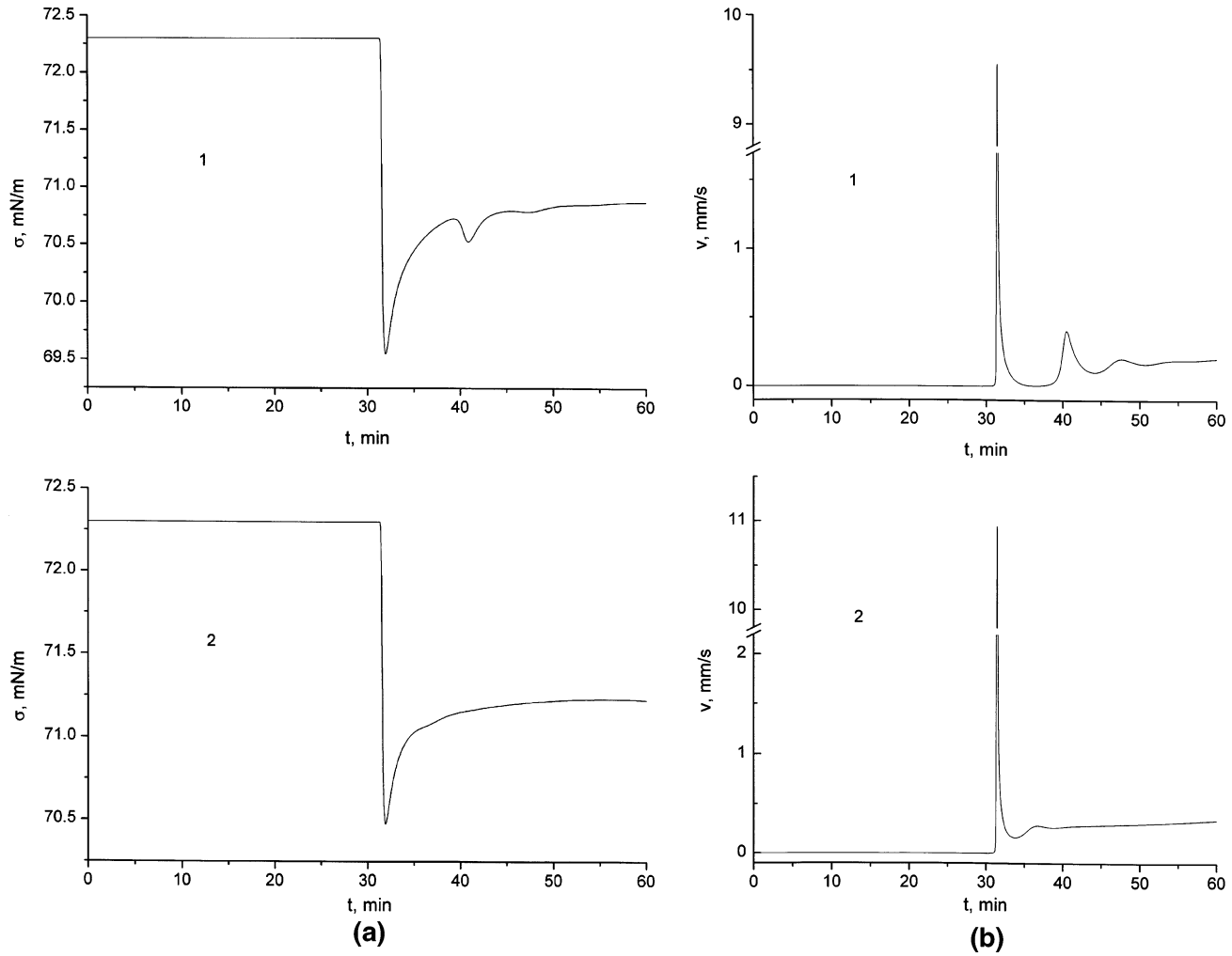

Figure 6. Graphical depictions of (a) surface tension σ versus time t and (b) surface velocity v versus time t for $H = 20$ mm and $h = 8$ mm: curve 1, $R = 25$ mm, and curve 2, $R = 30$ mm.

TABLE 4: Dependence of Supply and Loss of Surfactant during the Oscillation on the Cell Radius[a]

R, mm	surfactant supply, 10^{-9} mol	surfactant supply per surface unit, 10^{-11} mol/cm^2	surfactant loss, 10^{-9} mol	surfactant loss per surface unit, 10^{-11} mol/cm^2	surfactant loss to supply, %	surface tension decrease per oscillation, mN/m
20	1.40	11.16	1.22	9.75	87	0.42
25	1.75	8.90	1.56	7.90	89	0.24
30	1.92	6.78	1.76	6.22	92	0.14

[a] Immersion depth of the capillary was $h = 12$ mm.

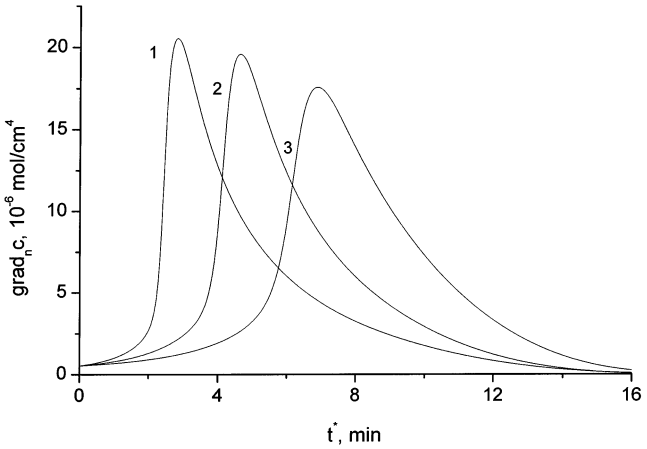

Figure 7. Normal concentration gradient near the surface in the vicinity of the capillary versus time *t*, depending on the cell radius: curve 1, $R = 30$ mm, $t = t^* + 283$ min, 41 s; curve 2, $R = 25$ mm, $t = t^* + 295$ min, 7 s; and curve 3, $R = 20$ mm, $t = t^* + 310$ min. Calculations were made for the capillary immersion depth $h = 12$ mm and the height of the liquid layer $H = 20$ mm; data are for the sixth oscillation.

oscillation appears in the system. The critical value of the cell radius is dependent on the capillary immersion depth. It was shown in the previous paragraph that, at $h = 6$ mm and $R = 20$ mm, the system displays a single oscillation, whereas repeated oscillations occur at $h = 8$ mm and $R = 20$ mm (Figure 1). The repeated oscillations still exist at $h = 8$ mm and $R = 22.5$ mm; however, the attained value of the negative velocity is already lower than that at $R = 20$ mm (Table 3). A further increase of the cell radius up to 25 mm is sufficient for the transition to only a single oscillation at $h = 8$ mm.

It is interesting to follow the system evolution at $h = 8$ mm and $R = 25$ mm. In this case, a reverse convective roll appears near the wall but it is too weak and cannot expand up to the capillary region. The maximum propagation of the reverse convective roll for $h = 8$ mm and $R = 25$ mm is shown in Figure 3a. Near the capillary, the liquid constantly moves upward. Therefore, the solute from the droplet region is continuously supplied to the surface supporting the concentration gradient that is directed from the capillary to the wall and the convective motion in this direction. If the cell radius decreases to 22.5 mm, the reverse convective roll extends to the capillary (Figure 3b). In this case, the liquid moves upward only near the upper portion of the capillary and it moves downward near the droplet. Thus, in this case, solute is not supplied from the droplet to the surface. The convective motion is rapidly dampened, and the system returns to a state where the diffusion transfer of the solute from the droplet to the surface is significant. Thus, it can be concluded that, for the generation of repeated oscillations, it is insufficient if only a reverse convective roll exists near the wall. It is necessary that the reverse roll extend upward to the capillary and break the supply of surfactant to the surface in the capillary region.

The appearance of the reverse convective roll at $h = 8$ mm and $R = 25$ mm does not lead to regular repeated oscillations; however, it still affects the system evolution. The system displays a pair of weak oscillations of the surface tension and of the velocity after the first oscillation, in contradiction to systems with higher *R* values, such as $h = 8$ mm and $R = 30$ mm, where the reverse roll does not appear at all (Figure 6).

TABLE 5: Dependence of the Auto-oscillation Characteristics on the Cell Depth

H, mm	induction period, min	Oscillation		maximum positive velocity value,[b] mm/s	surface tension decrease per oscillation,[a] mN/m
		period,[a] min	amplitude,[b] mN/m		
12	31	36	2.9/2.7	6.8/0.67	0.41
15	31	34	3.8/3.1	7.0/0.75	0.37
20	31	36	4.3/3.4	7.4/0.79	0.35
30	31	38	4.4/3.6	7.4/0.80	0.34

[a] Mean value for the third to sixth oscillations. [b] Value in the numerator represents that for the first oscillation, whereas the value in the denominator represents the mean value for the third to sixth oscillations.

During the induction period, surfactant accumulates mainly in the vicinity of the capillary and its concentration near the wall is approximately zero. Thus, the system behavior should be independent of the horizontal dimensions at this period of time.[7] As expected, the cell radius does not affect the induction period. At the same time, the oscillation period decreases as the cell radius increases for the two considered values of the immersion depth of the capillary. The main cause is the acceleration of the processes with the increase of the cell radius and, particularly, the increase of the growth rate of the velocity.

The amplitude of the oscillations decreases as the cell radius increases, because of the increasing surface area. At the same time, both the normal concentration gradient near the surface and the total amount of surfactant supplied to the surface during the oscillation increase as the cell radius increases (see Figure 7 and Table 4). The amount of surfactant removed from the surface during the process of a gradual increase of the surface tension also increases as the cell radius increases. The percentage of surfactant that is removed from the surface increases as the radius increases. Therefore, the mean value of the surface tension decreases more rapidly with time in cells of smaller radius. This phenomenon is observed from the decrease of the surface tension per oscillation.

Cell Depth. The changes in the cell depth affect the auto-oscillation characteristics less than changes in the capillary immersion depth or cell radius (Table 5). The induction period and the oscillation period are almost independent of this parameter. The amplitude of the oscillation, as well as the surface velocity, increase as the cell depth increases. The dependence is almost insignificant at large cell depths. The mean value of the surface tension decreases rather weakly as the cell depth increases.

Droplet and Capillary Radii. The effect of the droplet and capillary radii on the auto-oscillation characteristics is observed from the data given in Table 6. The variation of these parameters shows that changes in the induction period and oscillation period

TABLE 6: Dependence of Auto-oscillation Characteristics on the Droplet and the Capillary Radii

droplet radius, mm	capillary radius, mm	induction period, min	Oscillation		maximum positive velocity value,[b] mm/s	surface tension decrease per oscillation,[a] mN/m
			period,[a] min	amplitude,[b] mN/m		
1	1	33	37	1.9/1.7	6.0/0.86	0.15
1.25	1	32	36	3.3/2.8	6.9/0.82	0.26
1.5	1	31	36	4.3/3.4	7.4/0.79	0.35
1.75	1	31	38	5.4/4.2	7.8/0.78	0.46
2	1	31	39	6.3/4.8	8.0/0.77	0.55
2	1.5	31	34	5.8/3.9	7.0/0.69	0.47
2	2	32	33	4.1/2.6	5.5/0.60	0.32

[a] Mean value for the third to sixth oscillations. [b] Value given in the numerator represents that for the first oscillation, whereas the value given in the denominator represents the mean value for the third to sixth oscillations.

are insignificant. The oscillation amplitude increases noticeably as the droplet radius increases, according to the increase of the interfacial area where the surfactant dissolves. For the same reason, the oscillation amplitude decreases as the capillary radius increases. The mean value of the surface tension decreases faster for larger droplets and thinner capillaries. In contrast to other geometrical parameters, an increase of the droplet radius leads to an increase of the oscillation amplitude, even for a small decrease in the surface velocity (for the second and subsequent oscillations).

Comparison with Experimental Data. Comprehensive experimental investigation of the geometry effects on the auto-oscillation characteristics has been performed for the heptanol−water system.[19] The main difference between this experimental system and that considered previously is attributed to the important role of the buoyancy, because the density of the heptanol solution is less than that of water, which is not considered in the present theoretical study. This seems to be the most probable reason for the discrepancy between the experimental and numerical results, in regard to the dependence of the auto-oscillation characteristics on the immersion depth of the capillary. The calculations predict an increase of the period and a decrease of the amplitude with the increase of the immersion depth of the capillary, whereas any noticeable dependence of these characteristics on the capillary immersion depth was not found in the experiments. There is also a discrepancy between calculated and experimentally observed dependence of the oscillation period on the cell radius that can be as well attributed to the effect of the buoyancy-driven convection in the heptanol−water system.

On the other hand, the experimental studies of the octanol−water system show a dependence of the auto-oscillation characteristics on the immersion depth of the capillary. The enumerical simulations of the octanol−water system predict the existence of a critical immersion depth of the capillary and provides values for the critical depth that are rather similar to those of the experiments with this system (for a cell radius of 22.5 mm, a value of $h_c = 5.5$ mm was obtained in the experiments;[4] a value of $h_c = 8$ mm was calculated by the theory). The theoretical prediction of the proportionality of the critical immersion depth, relative to the cell radius, and the decrease of the oscillations amplitude with increases in the cell radius are also in agreement with the experimental observations.[4,19] The dependence of the oscillations characteristics on the droplet radius also agrees with the experiments.

Conclusions

Numerical simulations of the behavior of the model system that represents a surfactant droplet, which dissolves at the tip of the capillary under the liquid−gas interface in a cylindrical cell with rigid walls, are performed for different cell dimensions, capillary immersion depths, and capillary and droplet radii. In the mathematical model, it is assumed that both diffusion surfactant transfer, because of its nonuniform distribution, and convective transfer, caused by the gradient of the surface tension (Marangoni effect), occur in the system. Both processes are coupled with adsorption/desorption at the gas−liquid interface. The development of repeated auto-oscillations in this system is attributed to the interaction of the surface concentration wave with the lateral container wall, resulting in the formation of a convective flow in the opposite direction. That is the reason why the oscillation characteristics are strongly dependent on the system geometry.

The induction period is less affected by the system geometry. The induction period increases strongly as the immersion depth of the capillary increases, but it is dependent only very insignificantly on the droplet and the capillary radii and is practically independent of the cell dimensions.

The oscillation period is dependent mainly on the capillary immersion depth and the cell radius. In the framework of the used model, it was established that the increase of the cell radius affects the system behavior in a manner similar to that of a decrease in the capillary immersion depth. Namely, it leads to a decrease of the oscillations period. Repeated oscillations do not appear in the system if the cell radius exceeds a certain critical value (for a given immersion depth of the capillary) or the immersion depth of the capillary is lower than a certain critical value (by a given cell radius). Therefore, the ratio of the cell radius to the immersion depth of the capillary (the aspect ratio) is the most important geometrical parameter.

The amplitude of the auto-oscillation is affected by all the geometrical parameters. The amplitude increases as the droplet radius and the cell depth each increase and decreases as the immersion depth of the capillary and the radii of the cell and the capillary increase.

The existence of a critical aspect ratio—a value that, when exceeded, repeated oscillations do not appear in the system—is confirmed by the experimental data. The same good agreement between the results of the theoretical calculations and the experimental findings exists for the decrease of the oscillations amplitude with the increase of the cell radius and with the decrease of the droplet radius, as well as for the independence of both the oscillations period and the induction period of the droplet radius. Certain discrepancies in the theoretical and experimental dependencies of the oscillation characteristics on the capillary immersion depth and cell radius are most probably related to the effect of buoyancy.

The study of the effects of system geometry on the characteristics of the surface tension auto-oscillation allows for a better understanding of the mechanism of this phenomenon. The theoretical simulations substantiate that the diffusion mass transfer dominates during the induction period, and, particularly,

the concentration gradients attained in the system at the end of the induction period are crucial for the development of instability, whereas the velocity values that were attained have only a minor role during this time. It is shown that, during the induction period, the surface tension can remain constant by diffusion-controlled adsorption kinetics, when hydrodynamic instability begins in the system at sufficiently small values of the surface concentration (outside the experimental detection limit).

The conditions for the development of repeated oscillations are defined more precisely. For the system to return to the slow (diffusion) state and, thus, generate repeated oscillations, it is insufficient if only a reverse convective roll develops near the wall; the reverse roll must extend upward to the capillary and break the supply of surfactant to the surface in the capillary region.

Acknowledgment. N.M.K. gratefully thanks the Max-Planck-Institute of Colloids and Interfaces for the financial support of this work.

References and Notes

(1) Glansdorf, P.; Prigogine, I. *Thermodynamic Theory of Structure, Stability and Fluctuations*; Wiley: London, 1971.

(2) Zieper, J., Oertel, H., Eds. *Convective Transport and Instability Phenomena*; Braun: Karlsruhe, Germany, 1982.

(3) Kovalchuk, V. I.; Kamusewitz, H.; Vollhardt, D.; Kovalchuk, N. M. *Phys. Rev. E* **1999**, *60*, 2029.

(4) Kovalchuk, N. M.; Vollhardt, D. *J. Phys. Chem. B* **2000**, *104*, 7987.

(5) Kovalchuk, N. M.; Kovalchuk, V. I.; Vollhardt, D. *Phys. Rev. E* **2001**, *63*, 031604.

(6) Kovalchuk, N. M.; Vollhardt, D. *J. Phys. Chem. B* **2001**, *105*, 4709.

(7) Kovalchuk, N. M.; Vollhardt, D. *Phys. Rev. E* **2002**, *66*, 026302.

(8) Dupeyrat, M.; Nakache, E. *Bioelectrochem. Bioenerg.* **1978**, *5*, 134.

(9) Magome, N.; Yoshikava, K. *J. Phys. Chem.* **1996**, *100*, 19102.

(10) Arai, K.; Kusu, F. In *Liquid Interfaces in Chemical, Biological and Pharmaceutical Applications*; Volkov, A. G., Ed.; Surfactant Science Series 95; Marcel Dekker: New York, 2001.

(11) Maeda, K.; Nagami, S.; Yoshida, Y.; Ohde, H.; Kihara, S. *J. Electroanal. Chem.* **2001**, *496*, 124.

(12) Takahashi, T.; Yui, H.; Sawada, T. *J. Phys. Chem. B* **2002**, *106*, 2314.

(13) Koschmieder, E. L.; Prahl, S. A. *J. Fluid Mech.* **1990**, *215*, 571.

(14) Ondarçuhu, T.; Millan-Rodriguez, J.; Mancini, H. L.; Garcimartin, A.; Perez-Garsia, C. *Phys. Rev. E* **1993**, *48*, 1051.

(15) Daubi, P. C.; Lebon, G. *J. Fluid Mech.* **1996**, *329*, 25.

(16) Daubi, P. C.; Lebon, G.; Bouhy, E. *Phys. Rev. E* **1997**, *56*, 520.

(17) Monti, R.; Savino, R.; Lappa, M. *Acta Astronaut.* **2000**, *47*, 753.

(18) Linde, H.; Velarde, M. G.; Wiershem, A.; Waldheim, W.; Loeschke, K.; Rednikov, A. Y. *J. Colloid Interface Sci.* **1997**, *188*, 16.

(19) Grigorieva, O. V.; Kovalchuk, N. M.; Grigoriev, D. O.; Vollhardt, D., submitted to *ChemPhysChem*.